Available online at www.sciencedirect.com

ScienceDirect

Procedia CIRP 55 (2016) 65 – 70

www.elsevier.com/locate/procedia

5th CIRP Global Web Conference Research and Innovation for Future Production

Effect of Current Efficiency on Electrochemical Micromachining by Moving Electrode

V.M. Volgin[a,*], V.V. Lyubimov[a], I.V. Gnidina[a], A.D. Davydov[b], T.B. Kabanova[b]

[a]*Tula State University, pr. Lenina 92, Tula 300012, Russia*
[b]*Frumkin Institute of Physical Chemistry and Electrochemistry RAS, Leninskii pr. 31, Moscow 119071, Russia*

* Corresponding author. Tel.: +7-4872-35-24-52; fax: +7-4872-35-81-81. *E-mail address:* volgin@tsu.tula.ru

Abstract

In this work, the effect of current efficiency on the electrochemical micromachining by moving electrode is studied theoretically. The Laplace equation for the electric potential and the equation of workpiece surface evolution are used as the mathematical model of the process. A new scheme of solution of free boundary problem for steady-state electrochemical micromachining is proposed. According to the scheme, the initial approximation of the workpiece surface is prescribed. In the course of modeling, the workpiece surface moves in the normal direction at a rate proportional to the discrepancy of the steady-state condition. The effect of various dependences of current efficiency on the local current density is analyzed. As a result of simulation, the dependences of the shape and sizes of machined surface on the current efficiency and the machining parameters are obtained.

Peer-review under responsibility of the scientific committee of the 5th CIRP Global Web Conference Research and Innovation for Future Production

Keywords: Electrochemical micromachining; Current efficiency; Numerical simulation

1. Introduction

Along with the methods of mechanical, chemical, and physical treatment, various schemes of electrochemical micromachining (ECMM) are used to fabricate complex-shaped and microstructured surfaces [1]. ECMM offers several advantages: the absence of mechanical and heat effects on the workpiece (WP), no tool wear, relatively high material removal rate, smooth and bright surface, and the production of components of complex geometry [2, 3]. Therefore, ECMM is used in many industrial applications including turbine blades, engine castings, bearing cages, gears, dies and molds and surgical implants [3].

The following schemes of electrochemical machining are widely used: (1) with the use of a stationary non-profiled tool-electrode (TE) and a mask placed on the anode [4, 5] or cathode [6]; (2) with a profiled TE moving towards the workpiece surface [7]; (3) with non-profiled TE, which moves along the workpiece surface by the prescribed trajectory with the aid of numerically controlled system [8]. The term “non-profiled” means that the shape and sizes of TE do not correspond to the targeted shape of workpiece surface. In recent years, ECMM by moving electrode has attracted increasing interest, especially for machining of complex-shaped microworkpieces [9]. The shape and sizes of the machined surface depend on a large number of factors; therefore, a precise prediction of the geometry of workpiece surface is of great practical importance [10]. In the general case, the shape and sized of machined surface can be determined by solving the non-steady-state problem [11, 12]. However, the solution of non-steady-state problem requires a large volume of computation. Frequently, the quasi-steady state is reached in a short time, i.e. in the system of coordinates related to the TE, the shape and sizes of the workpiece do not change with the time. In this case, ECMM can be simulated using the models of steady-state shaping [13, 14]. Within the approximation of “ideal” ECMM process, the determination of steady-state shape of workpiece surface is reduced to the solution of free boundary problem for the Laplace equation. The condition of steady state [13] or the condition of constant current density [14] is used as an additional condition. In some cases (point, rectangular, corner

Peer-review under responsibility of the scientific committee of the 5th CIRP Global Web Conference Research and Innovation for Future Production
doi:10.1016/j.procir.2016.08.031

TE, etc.), the exact analytical [14] or approximate numerical [15] solution of the problem of steady-state ECMM can be obtained. In most cases, even for the cylindrical TE, the solution of steady-state problem requires the non-steady-state methods. This complicates considerably the prediction of the shape and sizes of machined surface.

The current efficiency depends on the local current density and has a pronounced effect on the shape and dimensions of workpiece surface. In several works [16, 17], it was shown that, when the current efficiency has the form of a step function of current density, the accuracy of ECMM increases significantly. However, the effect of variable current efficiency on the electrochemical machining by moving electrode has not been adequately investigated.

The aim of this work is to develop an effective method for modeling steady-state ECMM by moving TE of arbitrary shape that takes into account the dependence of current efficiency on the current density.

2. Mathematical model

An “ideal” model for ECMM by moving TE is considered (Fig. 1a). The following basic assumptions are made: 1) there are no concentration or temperature gradients within the electrode gap due to the intense electrolyte solution flow; 2) the dependence of current on the electrode potential is ignored. Under these assumptions, the primary distribution of potential and current density takes place, Faraday's law of electrolysis can be employed to determine the rate of the workpiece dissolution:

$$\operatorname{div}(\operatorname{grad}\varphi)=0, \tag{1}$$

$$\mathbf{i}=-\chi\operatorname{grad}\varphi, \tag{2}$$

$$v_n=\eta\varepsilon_V\mathbf{i}\cdot\mathbf{n}, \tag{3}$$

where φ is the potential; χ is the conductivity of electrolyte solution; $\mathbf{i}$ is the current density; $\mathbf{n}$ is a unit vector of outer normal to the workpiece surface; ε_V is the volumetric electrochemical equivalent of the workpiece material; η is the current efficiency; v_n is the rate of electrochemical dissolution.

The following boundary conditions are used:

$$\varphi|_{\mathrm{WP}}=u, \tag{4}$$

$$\varphi|_{\mathrm{TE}}=0, \tag{5}$$

$$(\partial\varphi/\partial n)_{\mathrm{I}}=0, \tag{6}$$

where u is the applied voltage; subscripts WP, TE, and I denote workpiece, tool-electrode and isolator, respectively.

In the two-dimensional case, in the system of coordinates related to the TE, the equation of the workpiece surface evolution $y_{\mathrm{WP}}(x,t)$ can be presented in the following form:

$$\frac{\partial y_{\mathrm{WP}}}{\partial t}=-v_n\sqrt{1+\left(\frac{\partial y_{\mathrm{WP}}}{\partial x}\right)^2}+v_{\mathrm{TE}}, \tag{7}$$

where t is the time; v_{TE} is the feed rate of tool-electrode.

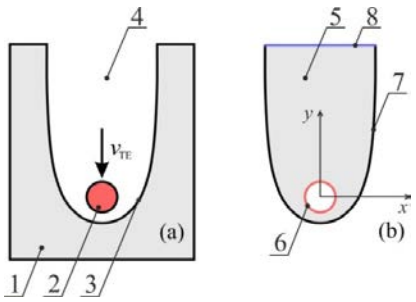

Fig. 1. (a) Scheme of electrochemical micromachining by moving tool-electrode and (b) the computational region: (1) workpiece, (2) TE that moves towards the workpiece at a rate v_{TE}; (3) workpiece surface; (4) interelectrode gap filled with the electrolyte solution; (5) computational region; (6) surface of moving TE; (7) machined surface; and (8) insulator surface that bounds the computational region.

In the steady state, equation (7) takes the following form:

$$\eta\varepsilon_V\chi\frac{\partial\varphi}{\partial n}+v_{\mathrm{TE}}n_y=0, \tag{8}$$

where $n_y=-\cos\alpha=-1/\sqrt{1+(\partial y_{\mathrm{WP}}/\partial x)^2}$ is the projection of a unit vector of the outer normal to the workpiece surface onto the y axis and α is an angle between the direction of tool-electrode feed and the outer normal to the workpiece surface.

For convenient solution and analysis of the results, the mathematical model is presented in the dimensionless form. The diameter of the circumcircle for the TE cross-section (d_{TE}) is taken as a unit length; the characteristic applied voltage ($d_{\mathrm{TE}}v_{\mathrm{TE}}/(\eta^*\varepsilon_V\chi)$), as a unit electric potential; and the characteristic current density ($v_{\mathrm{TE}}/(\eta^*\varepsilon_V)$), as a unit current density:

$$X=\frac{x}{d_{\mathrm{TE}}},\ Y=\frac{y}{d_{\mathrm{TE}}},\ \Phi=\frac{\eta^*\varepsilon_V\chi}{d_{\mathrm{TE}}v_{\mathrm{TE}}}\varphi,\ \mathbf{I}=\frac{\eta^*\varepsilon_V}{v_{\mathrm{TE}}}\mathbf{i},\ U=\frac{\eta^*\varepsilon_V\chi u}{d_{\mathrm{TE}}v_{\mathrm{TE}}}. \tag{9}$$

Here X,Y are the dimensionless coordinates; Φ is the dimensionless potential; $\mathbf{I}$ is the dimensionless current density; U is the dimensionless applied voltage.

$$\operatorname{div}(\operatorname{grad}\Phi)=0. \tag{10}$$

The boundary conditions:

$$\Phi|_{\mathrm{TE}}=0, \tag{11}$$

$$\Phi|_{\mathrm{WP}}=U, \tag{12}$$

$$\left(\frac{\eta}{\eta^*}\frac{\partial\Phi}{\partial N}+N_Y\right)\Big|_{\mathrm{WP}}=0, \tag{13}$$

$$(\partial\Phi/\partial N)_{\mathrm{I}}=0. \tag{14}$$

The mathematical model (10) – (14) involves one dimensionless parameter U, one dimensionless function η/η^* that prescribes the dependence of current efficiency on the current density, and preliminarily unknown workpiece surface $Y_{\mathrm{WP}}(X)$. Dimensionless parameter U has a physical meaning:

it is a ratio of the steady-state frontal interelectrode gap in the case of machining by a plane TE $s_F = \eta^* \varepsilon_V \chi u / v_{\text{TE}}$ to the diameter of TE, i.e. $U = s_F / d_{\text{TE}} = S_F$. Parameter S_F was used in the previous work [11]. Obviously, the results obtained at equal values of S_F [11] and U (here) should coincide.

When choosing the function η / η^*, it is taken into account that, at a constant current efficiency, in the point where $N_Y = -1$, the derivative $\partial\Phi / \partial N$ takes the largest value (equal to unity). Taking into account that the dimensionless current density is defined as $I = \partial\Phi / \partial N$, the dependence of the current efficiency on the current density can be prescribed as a function of dimensionless current density that varies from 1 to 0. For the sake of definiteness, the smoothed step function is used. It is described by the following equations:

$$\frac{\eta}{\eta^*} = \begin{cases} \eta_L, \text{ if } I < I^* - \delta I^*, \\ \eta_L + \dfrac{\eta_H - \eta_L}{2\delta I^*}\left(I - I^* + \delta I^*\right), \text{if } I^* - \delta I^* < I < I^* + \delta I^*, \\ \eta_H, \text{ if } I > I^* - \delta I^*, \end{cases} \quad (15)$$

where I^* is the dimensionless current density corresponding to the middle of the zone of linear dependence of current efficiency on the current density; δI^* is the half width of the zone of linear dependence of current efficiency on the current density; η_L is the current efficiency at low dimensionless current density; and η_H is the current efficiency at high dimensionless current density.

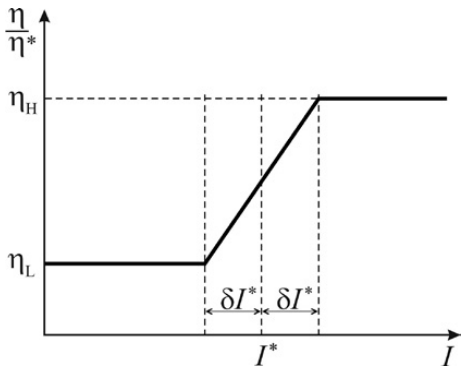

Fig. 2. Piecewise dependence of current efficiency on dimensionless current density.

The problem will be solved using the pseudo-transient method. From equation (13), it follows that, in the steady state, the rates of the motion of a workpiece surface point in the direction of its outer normal due to the anodic dissolution $\left(\eta / \eta^* \partial\Phi / \partial N\right)$ and due to the feed of TE $\left(N_Y\right)$ are equal. This condition can be modified as follows:

$$V_{\text{WP}} = \frac{\eta}{\eta^*}\frac{\partial\Phi}{\partial N} + N_Y, \quad (16)$$

where V_{WP} is the normal component of the workpiece surface rate.

In view of equation (16), we can write:

$$\frac{dX_{\text{WP}}}{d\tau} = N_X V_{\text{WP}} = N_X\left(\frac{\eta}{\eta^*}\frac{\partial\Phi}{\partial N} + N_X\right), \quad (17)$$
$$\frac{dY_{\text{WP}}}{d\tau} = N_Y V_{\text{WP}} = N_Y\left(\frac{\eta}{\eta^*}\frac{\partial\Phi}{\partial N} + N_Y\right),$$

where τ is the dimensionless time.

Thus, to determine the steady-state shape of workpiece surface, it is necessary to solve the systems of equations (10) and (17) with boundary conditions (11), (12) and (14) until the steady-state solution is obtained.

3. Results and discussion

In the dimensionless variables, the equation of the workpiece surface during non-steady-state ECMM (7) can be written in the following form:

$$N_Y \frac{\partial Y_{\text{WP}}}{\partial\tau} = \frac{\eta}{\eta^*}\frac{\partial\Phi}{\partial N} + N_Y. \quad (18)$$

Equation (18) enables one to determine the variation of the shape and dimensions of workpiece surface in the course of machining. The right-hand side of equation (18), as well as the right-hand sides of equations (17), involves V_{WP}, which is determined by equation (16). However, equation (18) and proposed equations (17) exhibit a number of significant distinctions: (1) Equation (18) enables one to calculate the values of Y_{WP} at the given values of independent variable X, whereas equations (17) enable one to calculate new coordinates of a point of workpiece surface X_{WP} and Y_{WP}, which corresponds to the parametric representation of workpiece surface. (2) In accordance with equation (18), the points, which are located sufficiently far away from TE, move in the vertical direction at a rate equal to unity, whereas from equation (17), it follows that the point's motion rate steeply decreases with the distance from TE. (3) On the WP areas, where N_Y is low, equation (18) is stiff equation, which complicates significantly its solution.

As a result of above distinctions, during the solution of non-steady-state problem (18), the dimensions of computational region permanently increase, even after the completion of transient process and the formation of the steady-state distribution of interelectrode gaps near TE. This leads to the necessity of permanent remeshing of the grid of the boundary or finite elements. At the same time, when the proposed conditions (17) are used, the shape and dimensions of computational region change only in the case of deviation from the condition of steady state (Fig. 3).

Any shape of workpiece surface can be prescribed as the initial approximation (Fig. 3a). In the course of modeling, the shape and dimensions of workpiece surface varied starting from the region adjacent to the tool-electrode (Fig. 3b). The changes gradually propagated over the entire workpiece surface (Fig. 3c). As a result, the steady-state shape of anodic surface formed (Fig. 3d). Here, two points should be taken into account: the simplicity of prescribing the initial surface (for example, the boundary can be prescribed as a set of segments of straight lines and arcs of circles) and an extent of approaching actual machined surface (Fig. 3d). The closer is

the initial approximation to the required shape of the machined surface, the shorter is the time taken to solve the problem.

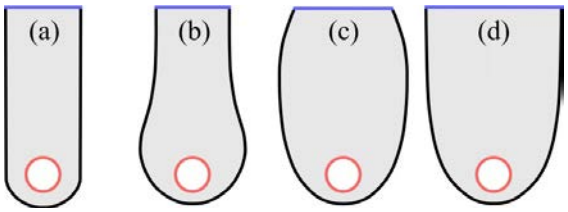

Fig. 3. (a) Initial computational region; (b) and (c) computational region in the course of pseudo-transient solution, and (d) computational region corresponding to the steady-state solution.

The numerical solution is performed stepwise. At each step (1) the Laplace equation (10) is solved numerically and the values of $(\partial\Phi/\partial N)_k^n$ in the computational grid points located at the boundary of computational region are determined; (2) equation (17) is solved numerically and new positions of the computational grid points located on the workpiece surface are determined:

$$(X_{\mathrm{WP}})_k^{n+1} = (X_{\mathrm{WP}})_k^n + \Delta\tau\left[N_X\left(\frac{\eta}{\eta^*}\frac{\partial\Phi}{\partial N} + (N_Y)\right)\right]_k^n, \qquad (19)$$

$$(Y_{\mathrm{WP}})_k^{n+1} = (Y_{\mathrm{WP}})_k^n + \Delta\tau\left[N_Y\left(\frac{\eta}{\eta^*}\frac{\partial\Phi}{\partial N} + (N_Y)\right)\right]_k^n,$$

where $\Delta\tau$ is the time step; k, n are subscripts denoting the number of boundary grid point and number of time step, respectively.

The numerical solution of the Laplace equation was performed by the boundary element method. The number of boundary elements, the time step, and the time of modeling were determined from the conditions of the absence of the effect of boundary element parameters on the numerical solution, the stability of numerical solution, and reaching the steady state. The numerical method was described in detail in previous works [11, 12].

The dimensionless total current is determined as the integral of the local current density over the workpiece surface:

$$I_{\mathrm{FULL}} = \int_{WP} I dL. \qquad (20)$$

The cut width is determined by the following equation:

$$H = \int_{\mathrm{WP}} \frac{\eta}{\eta^*} I dL = \int_{\mathrm{WP}} \frac{\eta}{\eta^*}\frac{\partial\Phi}{\partial N} dL. \qquad (21)$$

In the absence of side reactions, i.e. at 100% current efficiency, $H = I_{\mathrm{FULL}}$. When the current efficiency depends on the current density, the ratio

$$E = W / I_{\mathrm{FULL}} \qquad (22)$$

is the efficiency coefficient.

By the results of modeling, the dimensionless frontal interelectrode gap was determined:

$$S_{\mathrm{F}}^* = \min(Y_{\mathrm{TE}}) - \min(Y_{\mathrm{WP}}). \qquad (23)$$

The modeling was performed for the machining by a cylindrical moving tool-electrode. The surface of a groove with vertical parallel side walls and a bottom in the shape of a semicircle was taken as the initial approximation for the anode surface. The surface of insulator bounding the workpiece surface was taken to be flat (Fig. 3a).

The calculations were performed at various values of parameters of dependence of current efficiency on the current density (15) and dimensionless parameter U. Figs. 4 – 7 give the results of modeling.

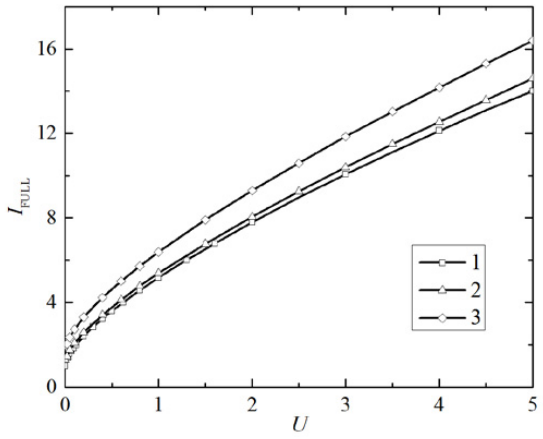

Fig. 4. Dependences of total current on parameter U at $\eta_L = 0$, $\eta_H = 1$: (1) $I^* = 0$ (a constant current efficiency); (2) $I^* = 0.5$, $\delta I^* = 10^{-3}$; (3) $I^* = 1$, $\delta I^* = 10^{-3}$.

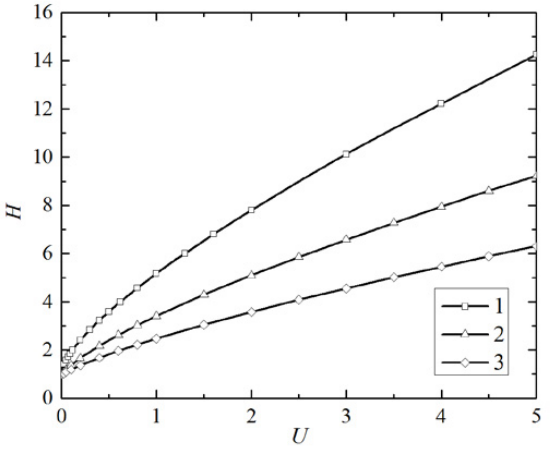

Fig. 5. Dependences of dimensionless cut width on parameter U at $\eta_L = 0$, $\eta_H = 1$: (1) $I^* = 0$ (a constant current efficiency); (2) $I^* = 0.5$, $\delta I^* = 10^{-3}$; (3) $I^* = 1$, $\delta I^* = 10^{-3}$.

The total current increases with increasing dimensionless applied voltage by the superliner dependence; thereby, the total current increases with increasing I^*, i.e. with decreasing fraction of surface, at which the anodic dissolution of workpiece material occurs. This is explained by a decrease of the cut width with a decrease of the current efficiency (Fig. 5) leading to a decrease of the ohmic resistance of electrolyte solution in the interelectrode gap and, consequently, to an increase of the total current.

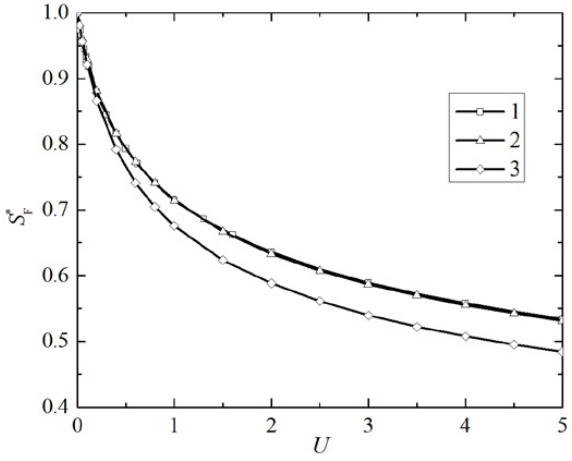

Fig. 6. Dependences of frontal gap on parameter U at $\eta_L = 0$, $\eta_H = 1$: (1) $I^* = 0$ (a constant current efficiency); (2) $I^* = 0.5$, $\delta I^* = 10^{-3}$; (3) $I^* = 1$, $\delta I^* = 10^{-3}$.

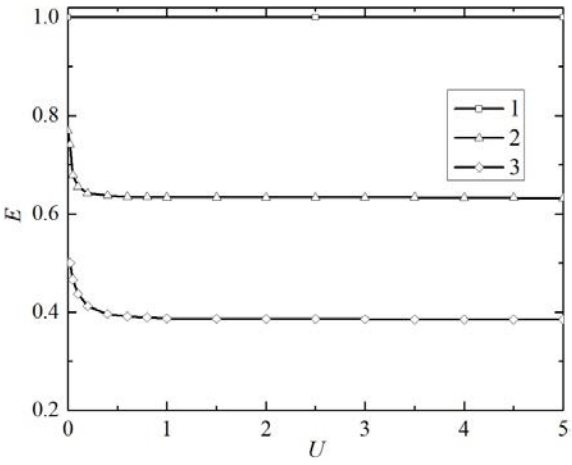

Fig. 7. Dependences of efficiency coefficient at $\eta_L = 0$, $\eta_H = 1$: (1) $I^* = 0$ (a constant current efficiency); (2) $I^* = 0.5$, $\delta I^* = 10^{-3}$; (3) $I^* = 1$, $\delta I^* = 10^{-3}$.

From the above results, it is seen that the current efficiency has a pronounced effect on the parameters of the machined surface. The effect on the cut width (Fig. 5) is stronger (it varies more than twofold) than on the frontal interelectrode gap (Fig. 6) (the frontal interelectrode gap is the shortest distance between the surfaces of the electrodes).

The current efficiency has a pronounced effect on the efficiency coefficient of ECMM (Fig. 7). At $I^* = 0$, E = 1; at $I^* = 0.5$, E varies from 0.77 to 0.63; and at $I^* = 1$, E varies from 0.5 to 0.39 when U increases from 0 to 5. Thus, ECMM at high current densities corresponding to the transition from the prevailing dissolution of workpiece material to the side electrochemical reactions, the efficiency coefficient can decrease by more than 50%.

Figs. 8 and 9 give the shapes of the surfaces machined at U=0.5 and various values of parameters of dependence of current efficiency on the current density. The surface of TE is shown with bold line; the center of the TE coincides with the origin of coordinates. In view of symmetry in the case of machining by cylindrical tool-electrode, Fig. 8 shows only a half of the workpiece surface. The effect of parameters of dependence of current efficiency on the current density on the shape and dimensions of the cut was investigated.

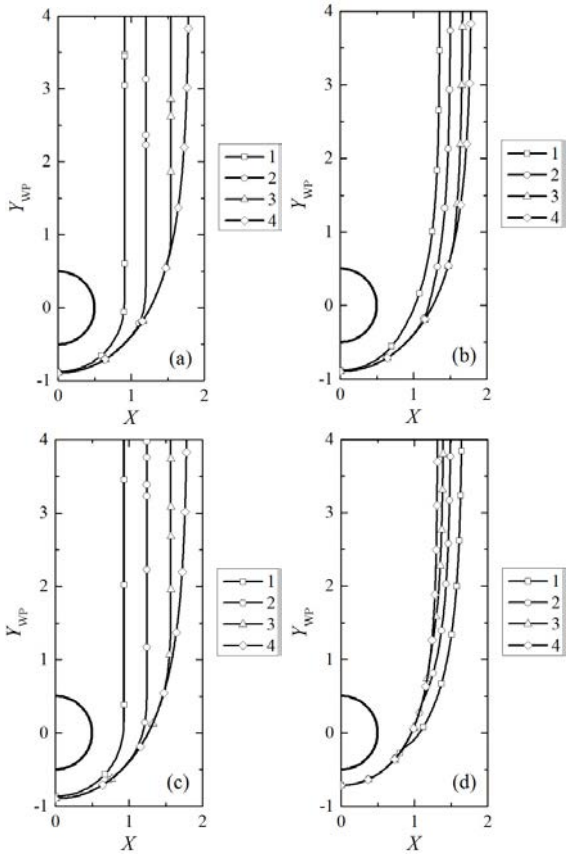

Fig. 8. Geometry of surface machined at U=0.5: (a) $\eta_L = 0$, $\eta_H = 1$, $\delta I^* = 10^{-3}$; (b) $\eta_L = 0.5$, $\eta_H = 1$, $\delta I^* = 10^{-3}$, (c) $\eta_L = 0$, $\eta_H = 1$, $\delta I^* = 0.2$, (d) $\eta_L = 1$, $\eta_H = 0.5$, $\delta I^* = 0.2$, (1) $I^* = 1$, (2) $I^* = 0.5$, (3) $I^* = 0.2$, and (4) $I^* = 0$ (a constant current efficiency).

Parameter I^* has the strongest effect. When I^* increases from 0 to 1, the cut width is approximately halved (curves 4, 1 in Figs. 8a and 8c). An increase in the width of the transient zone δI^* from 0.001 to 0.2 leads to an insignificant (about 2%) increase in the cut width (Figs. 8a and 8c). Parameters η_L

and η_H have a more pronounced effect (Figs. 8b and 8d). When η_L increases from 0 to 0.5, the smallest cut width increases by 50% from 1.82 to 2.72 (Fig. 8b, curve 1), and when *I** decreases from 1 to 0, the cut width increases. When η_L increases to 1 and η_H decreases to 0.5, the character of the effect of *I** changes: the cut width decreases with decreasing *I** (Fig. 8d).

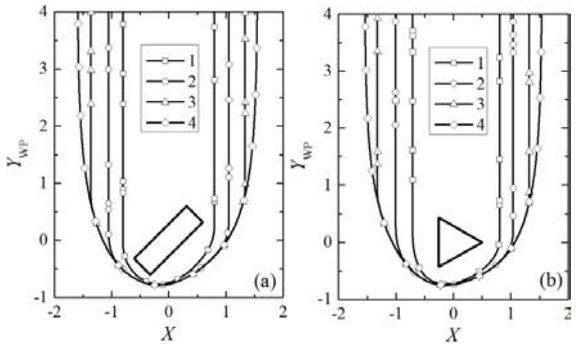

Fig. 9. Geometry of surface machined at U=0.5, $\eta_L = 0$, $\eta_H = 1$, $\delta I^* = 10^{-3}$: (a) rectangular TE; (b) triangular TE; (1) $I^* = 1$, (2) $I^* = 0.5$, (3) $I^* = 0.2$, and (4) $I^* = 0$ (a constant current efficiency).

To illustrate the potentialities of the proposed method, Fig. 9 gives the results of modeling for rectangular and triangular tool-electrodes.

4. Conclusions

The method for calculating the evolution of the shape and dimensions of a cavity in a workpiece machined by a moving tool-electrode in the shape of a rod with various (round or another) cross section at various dependences of the current efficiency on the current density is proposed and used.

The Laplace equation for the electric potential and the equation of workpiece surface evolution are used as the mathematical model of the process. A new scheme of solution of free boundary problem for steady-state electrochemical micromachining is proposed. According to this new scheme, the initial approximation of the workpiece surface is prescribed. In the course of modeling, the workpiece surface moves in the normal direction at a rate proportional to the discrepancy of the steady-state condition.

Acknowledgements

The reported study was funded by RFBR according to the research projects № 16-03-00786a, № 15-48-03250p_a and by the Ministry of Education and Science of the Russian Federation, Project no. 1096 of the Basic Part of the State Program.

References

[1] Rajurkar KP, Levy G, Malshe A, Sundaram MM, McGeough J, Hu X, Resnick R, DeSilva A. Micro and nano machining by electro-physical and chemical processes. CIRP Ann-Manuf Techn 2006;55(2):643-666.
[2] Datta M, Landolt D. Fundamental aspects and applications of electrochemical microfabrication. Electrochim Acta 2000;45:2535–2558.
[3] Rajurkar KP, Sundaram MM, Malshe AP. Review of electrochemical and electrodischarge machining. Procedia CIRP 2013;6:13-26.
[4] Datta M. Fabrication of an array of precision nozzles by through-mask electrochemical micromachining. J Electrochem Soc 1995;142(11): 3801-3805.
[5] Davydov AD, Kabanova TB, Volgin VM. Modeling of through-mask electrochemical micromachining. Chem Eng Trans 2014;41:85-90.
[6] Schonenberger I, Roy S. Microscale pattern transfer without photolithography of substrates. Electrochim Acta 2005;51(5):809-819.
[7] Forster R, Schoth A, Menz W. Micro-ECM for production of microsystems with a high aspect ratio. Microsyst Technol 2005;11(4-5):246-249.
[8] Kim BH, Ryu SH, Choi DK, Chu CN. Micro electrochemical milling. J Micromech Microeng 2005;5:124-129.
[9] Spieser A, Ivanov A. Recent developments and research challenges in electrochemical micromachining (μECM). Int J Adv Manuf Technol 2013;69(1-4):563-581.
[10] Davydov AD, Volgin VM, Lyubimov VV. Electrochemical machining of metals: Fundamentals of electrochemical shaping. Russ J Electrochem 2004;40:1230-1265.
[11] Volgin VM, Lyubimov VV, Kukhar VD, Davydov AD. Modeling of wire electrochemical micromachining. Procedia CIRP 2015;37:176-181.
[12] Volgin VM, Lyubimov VV, Davydov AD. Modeling of numerically controlled electrochemical micromachining. Chem Eng Sci 2016;140:252-260.
[13] Collett DE, Hewson-Browne RC, Windle DW. A complex variable approach to electrochemical machining problems. J Eng Math 1970;4(1):29-37.
[14] Karimov AKh, Klokov VV, Filatov EI. Methods of calculating electrochemical shaping. Kazan: Kazan University Press; 1990 [in Russian].
[15] Zhou Y, Derby JJ. The cathode design problem in electrochemical machining. Chem Eng Sci 1995;50(17):2679-2689.
[16] Zhitnikov VP, Oshmarina EM, Porechny SS, Fedorova GI. Limit model of electrochemical dimensional machining of metals. J Appl Mech Tech Phy 2014;55(4):718-725.
[17] Zhitnikov VP, Sherykhalina NM, Zaripov AA. Modelling of precision steady-state and non-steady-state electrochemical machining by wire electrode-tool. J Mater Process Tech 2016;235:49-54.